Published in "FEMS Yeast Research 14(5): 776–788, 2014"
which should be cited to refer to this work.

Characterization of yeast mutants lacking alkaline ceramidases *YPC1* and *YDC1*

Natalia S. Voynova[1], Shamroop K. Mallela[1], Hector M. Vazquez[1], Vanessa Cerantola[1], Mélanie Sonderegger[1], Jens Knudsen[2], Christer S. Ejsing[2] & Andreas Conzelmann[1]

[1]Department of Biology, University of Fribourg, Fribourg, Switzerland; and [2]Department of Biochemistry and Molecular Biology, University of Southern Denmark, Odense, Denmark

Correspondence: Andreas Conzelmann, Department of Biology, University of Fribourg, Ch. du Musée 10, CH-1700 Fribourg, Switzerland.
Tel.: +41 26 300 8631;
fax: +41 26 300 9735;
e-mail: andreas.conzelmann@unifr.ch

Present addresses: Natalia S. Voynova, Temasek Life Sciences Laboratory, National University of Singapore, Singapore City, Singapore
Vanessa Cerantola, Philip Morris Products SA, 2000 Neuchatel, Switzerland

Abstract

Humans and yeast possess alkaline ceramidases located in the early secretory pathway. Single deletions of the highly homologous yeast alkaline ceramidases *YPC1* and *YDC1* have very little genetic interactions or phenotypes. Here, we performed chemical-genetic screens to find deletions/conditions that would alter the growth of *ypc1*Δ*ydc1*Δ double mutants. These screens were essentially negative, demonstrating that ceramidase activity is not required for cell growth even under genetic stresses. A previously reported protein targeting defect of *ypc1*Δ could not be reproduced and reported abnormalities in sphingolipid biosynthesis detected by metabolic labeling do not alter the mass spectrometric lipid profile of *ypc1*Δ*ydc1*Δ cells. Ceramides of *ypc1*Δ*ydc1*Δ remained normal even in presence of aureobasidin A, an inhibitor of inositolphosphorylceramide synthase. Moreover, in caloric restriction conditions Ypc1p reduces chronological life span. A novel finding is that, when working backwards as a ceramide synthase *in vivo*, Ypc1p prefers C24 and C26 fatty acids as substrates, whereas it prefers C16:0, when solubilized in detergent and working *in vitro*. Therefore, its physiological activity may not only concern the minor ceramides containing C14 and C16. Intriguingly, so far the sole discernable benefit of conserving *YPC1* for yeast resides with its ability to convey relative resistance toward H_2O_2.

Keywords
secretion; chronological life span; vesicular traffic; synthetic genetic array; sphingolipid; aureobasidin A.

Introduction

Discovery of alkaline ceramidases in yeast

While mammalian cells contain acid, neutral and alkaline ceramidases residing in lysosomes, at the plasma membrane and in the early secretory pathway, respectively, only alkaline ceramidases have been described in yeast (Mao & Obeid, 2008). They go by the names of Ypc1p and Ydc1p (Fig. 1), are highly homologous over their entire sequence (54% identity) and reside in the ER, where also Lag1p and Lac1p, the two redundant acyl-CoA dependent ceramide synthases are located. Ypc1p and Ydc1p seem to be homeostatic enzymes, which cannot only hydrolyze ceramides into long chain base (LCB) and fatty acid, but also generate ceramides through the reverse reaction. Indeed, *YPC1* was discovered as a gene enabling cells, when overexpressed, to grow on fumonisin B1, a competitive inhibitor of Lag1p and Lac1p; its homolog *YDC1* was subsequently shown to have ceramidase activity also (Mao *et al.*, 2000a, b; Fig. 1). Similarly, in *lac1*Δ*lag1*Δ cells, LCBs accumulate and this renders the Ypc1p- or Ydc1p-mediated ceramide synthesis thermodynamically possible (Schorling *et al.*, 2001; Cerantola *et al.*, 2009). Yeast ceramidases Ypc1p and Ydc1p show slightly different substrate specificities: Ypc1p hydrolyzes ceramides containing phytosphingosine (PHS) or dihydrosphingosine (DHS), whereas Ydc1p is a dihydroceramidase, and this LCB specificity of Ydc1p is also observed for the reverse reaction (Mao *et al.*, 2000b; Cerantola *et al.*, 2009).

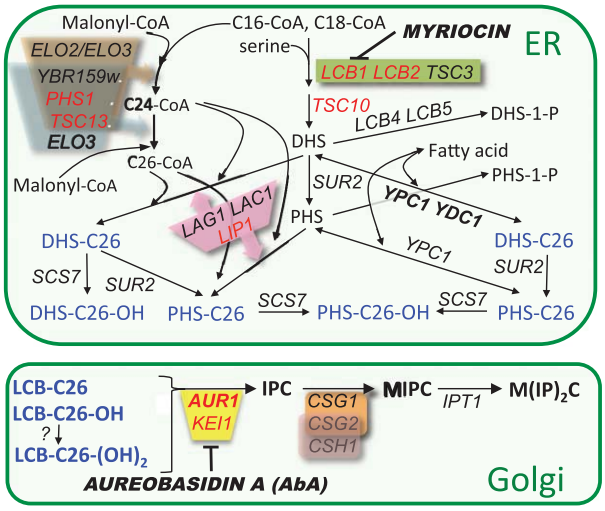

Fig. 1. Major pathways of sphingolipid biosynthesis in yeast. Gene names are in italic, essential genes in red and enzyme inhibitors in bold italics. A detailed description of the biosynthetic reactions can be found in recent reviews (Dickson *et al.*, 2006; Dickson, 2010).

Physiological expression levels of Ypc1p and Ydc1p

At their physiological expression levels, Ypc1p and Ydc1p markedly enhance growth of *lac1*Δ*lag1*Δ cells lacking acyl-CoA-dependent ceramide synthesis in that *lac1*Δ*lag1*Δ cells grow much better than *lac1*Δ*lag1*Δ*ypc1*Δ*ydc1*Δ (Cerantola *et al.*, 2009). Thus, even when expressed from their endogenous promoters, they may contribute to ceramide biosynthesis if Lac1p and Lac1p are not operational. Moreover, the reverse ceramidase activity of Ypc1p and Ydc1p in microsomal detergent extracts from wild-type (WT) cells can easily be detected and is quite substantial, as expression of *GAL1* promoter driven *YPC1*, placed on a 2 μ or a centromeric vector, increases the activity only 25 and 2.3-fold over WT levels, respectively (Mao *et al.*, 2000a; Ramachandra & Conzelmann, 2013; therein Supporting Information, Fig. S2d).

Impact of Ypc1p and Ydc1p on sphingolipid biosynthesis

The simultaneous presence of acyl-CoA-dependent ceramide synthases and alkaline ceramidases in the ER seems to create the potential for a futile circle. Indeed, in WT cells, the overexpression of *YPC1* and *YDC1* was shown to significantly increase the levels of free LCBs and LCB-phosphates and to reduce the biosynthetic flow of LCBs toward mature sphingolipids, whereas deletion of *YPC1* caused a significant increase of mature sphingolipids as detected by metabolic labeling with tritiated palmitate ([^{3}H]C16:0) or [^{3}H]serine (Mao *et al.*, 2000a, b). One also has to consider the possibility that ceramidases potentially generate biologically important alterations in the local sphingolipid composition of a membrane under certain circumstances, alterations that do not occur in *ypc1*Δ*ydc1*Δ (yyΔΔ) cells.

Aim of the study

It is likely that the Synthetic Genetic Array (SGA) studies performed in the past using *ypc1*Δ or *ydc1*Δ single mutants might have missed potential genetic interactions between a complete lack of alkaline ceramidase activity and other gene deletions because of potential paralog compensation between *YPC1* and *YDC1* (DeLuna *et al.*, 2008). We therefore did a chemical-genetic screen to find nonessential genes, which would impact the growth rate in the yyΔΔ background. We also followed up on a few published phenotypes of *ypc1*Δ or *ydc1*Δ cells and tested if they were exacerbated in yyΔΔ double mutant.

Materials and methods

Strains and growth conditions

Saccharomyces cerevisiae strains used are listed in Table S1, plasmids in Table S2. Mutant strains were generated using standard methods for crossing of single mutants, for plasmid transfection or for gene disruption using deletion cassettes generated by PCR. Cells were grown on rich medium (YPD or YPG) or synthetic complete media (yeast nitrogen base YNB, United States Biological) containing 2% glucose (D) or galactose (G) as a carbon source. Unless indicated otherwise, synthetic complete medium with 2% glucose was used.

Synthetic genetic arrays

Screens were performed according to published protocols (Collins *et al.*, 2010). The measurement of growth, the analysis and the visualization of high-throughput screen data were conducted with the help of the ScreenMill software (Dittmar *et al.*, 2010). A more detailed description of this and the following methods is to be found in the supporting information.

Fluorescence microscopy

For fluorescent imaging, cells were collected when in exponential phase at 30 °C unless indicated otherwise. Cells were imaged using an Olympus BX54 microscope equipped with a piezo-positioner (Olympus). Z sections (7–10 each 0.5 μm apart) were projected to

two-dimensional images and analyzed with the CellM software (Olympus).

Mass spectrometric lipid analysis

For Fig. 4a, lipids were extracted and analyzed in negative and positive ion mode by direct infusion mass spectrometry using an LTQ Orbitrap XL mass spectrometer equipped with the automated nanoflow ion source Triversa NanoMate (Advion Biosciences) as described (Ejsing *et al.*, 2006, 2009). For Fig. 5a and b, lipids were extracted and analyzed as described before (Hanson & Lester, 1980; Cerantola *et al.*, 2009) and inositolphosphorylceramide (IPC) and mannosyl-IPC (MIPC) lipids were identified based on release of characteristic fragment ions. Before injection, all lipid extracts were mixed with a fixed amount of lipid extract from WT cells grown in [^{13}C]glucose as the only carbon source and the data from different cell lines were made comparable by normalizing the signal intensities of this internal standard as a reference.

Triton X-100 solubilization assay

Crude membranes were isolated from early logarithmic cells by breaking cells with glass beads in ice-cold TNE-I buffer (50 mM Tris-HCl, pH 7.4, 150 mM NaCl, and 5 mM EDTA) supplemented with protease inhibitors (1 mM PMSF, 4 μM leupeptin, and 2 μM pepstatin) as described (Grossmann *et al.*, 2008). Debris was removed, and membranes were sedimented at 16 000 ***g*** for 75 min and resuspended in TNE-I buffer. For the determination of detergent resistance, aliquots corresponding to 50 μg of membrane protein in 100 μL TNE-I buffer were treated with increasing concentrations of Triton X-100 (0–0.8%) at room temperature for 30 min. The nonsolubilized material was sedimented by centrifugation (16 000 ***g*** at 4 °C for 30 min) and washed with 100 μL of detergent-free buffer.

The other methods used are described in the supporting information.

Results

Combining ceramidase deficiency with a further genetic deletion

The yyΔΔ, *ypc1*Δ and WT strains were robotically crossed with the 4978 individual strains of the nonessential deletion strain collection of *S. cerevisiae* in quadruplicate. Selected triple mutants were tested either on synthetic complete selection media or the same supplemented with 0.03 μg mL^{-1} of Aureobasidin A (AbA; Fig. 1), 25 μM PHS or 100 mM $CaCl_2$ or on media lacking inositol. The whole screen was carried out twice. Each *ypc1*Δ*ydc1*Δ*xxxX*Δ triple mutant was compared with the corresponding *xxxX*Δ single or *ypc1*Δ*xxxX*Δ double mutant to find *xxxX*Δ mutants, in which the deletion of *YPC1* and *YDC1* caused a growth phenotype. Twenty significant hits (P-value ≤ 0.05) were obtained and these were further verified by independent crosses and subsequent random sporulation analysis, tetrad analysis and serial dilution growth tests. None of the 20 could be validated through these further tests. While numerous *xxxX*Δ mutants were reproducibly resistant or hypersensitive to AbA, or PHS or $CaCl_2$, or to the absence of inositol, as reported before (Tani & Kuge, 2010, 2012; Young *et al.*, 2010) none of these altered sensitivities was exacerbated or mitigated in the *ypc1*Δ or yyΔΔ backgrounds. Yet, many more deletion mutants than previously reported (BIOGRID (http://thebiogrid.org/) were found to be AbA hypersensitive (N.S. Voynova and H. M. Vazquez, unpublished data).

Deletion of *YPC1* and *YDC1* does not affect the trafficking of Fus-Mid-GFP and other plasma membrane proteins

It has been recognized for some time that sphingolipids are required for trafficking of GPI anchored proteins (e.g. Gas1p) and many multispan membrane proteins (e.g. Pma1p) transiting through the secretory pathway to the plasma membrane or the vacuole (Horvath *et al.*, 1994; Bagnat *et al.*, 2000; Gaigg *et al.*, 2005). It is believed that targeting of many membrane protein requires association with sphingolipid- and ergosterol-rich subdomains of the membrane, which often are referred to as 'rafts'. Such proteins usually cannot be solubilized with nonionic detergents at 4 °C are said to be 'detergent resistant', a finding that in the past has been used as a proxy for potential raft association of proteins. A deletion strain library was screened microscopically for strains, in which the detergent resistant, chimerical Fus-Mid-GFP protein was not properly targeted to the plasma membrane (Proszynski *et al.*, 2005). Deletion of several enzymes metabolizing sphingolipids (*ELO3*, *SUR2*, *YPC1*; Fig. 1) or making ergosterol (ERG4, ERG6) caused Fus-Mid-GFP to accumulate in the Golgi or the vacuole. Deletion of *YPC1* provoked the accumulation of Fus-Mid-GFP in the Golgi. Expecting to see a stronger phenotype in yyΔΔ cells, we expressed the Fus-Mid-GFP construct of Proszynski *et al.* in our strains. In spite of numerous efforts, we observed no mislocalization of Fus-Mid-GFP neither in *ypc1*Δ cells nor in yyΔΔ cells (Fig. 2a), although we used the same genetic background and the same induction protocol as the original report (Proszynski *et al.*, 2005).

As shown in Fig. 2a, other raft-associated proteins such as Gas1p and Pma1p also were properly localized at the

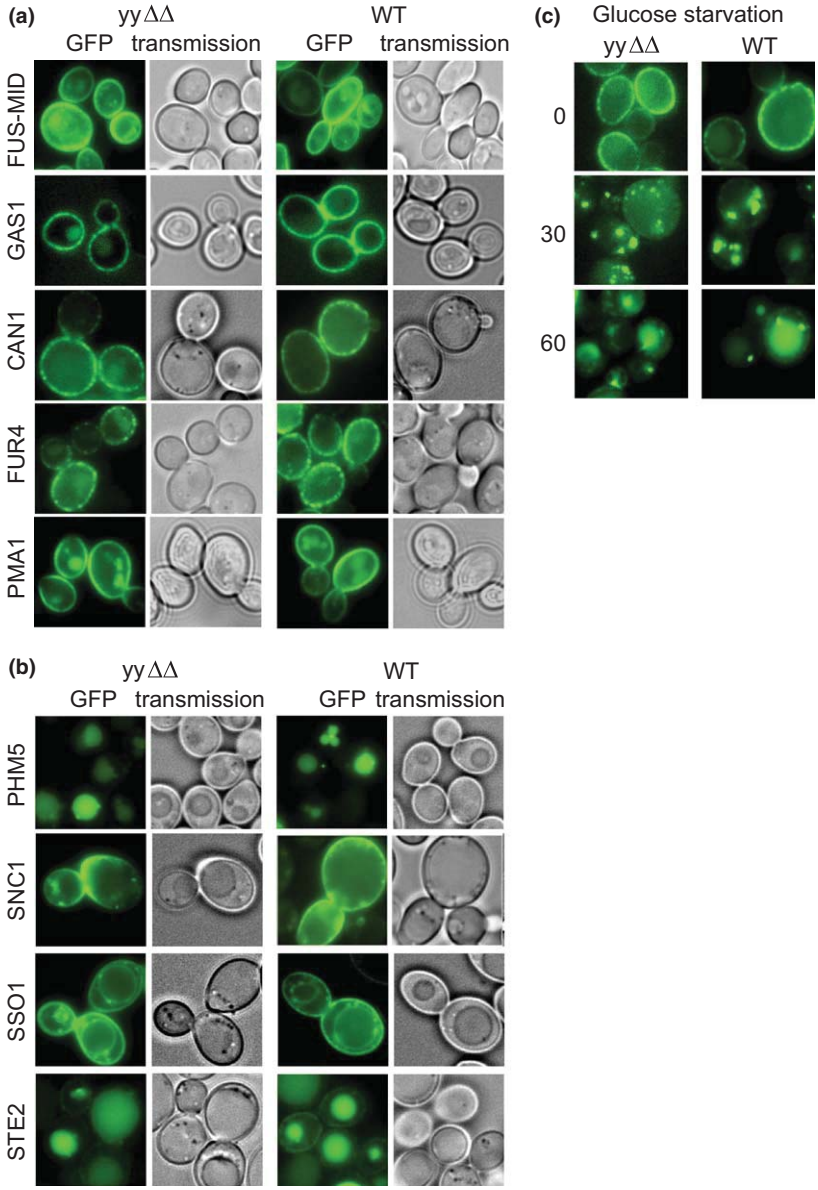

Fig. 2. Subcellular localization and organellar distribution of GFP-tagged membrane proteins. (a) WT and yyΔΔ cells expressing Fus-Mid-GFP behind the *GAL1* promoter were grown to mid-log phase on raffinose, then switched to galactose for 3 h at 30 °C prior to visualization by fluorescent microscopy as described (Proszynski *et al.*, 2005). Cells expressing GFP-tagged Gas1p, Can1p, Fur4p and Pma1p proteins under constitutive promoters were grown to the exponential phase before viewing. (b) WT and yyΔΔ cells expressing either of GFP-Phm5p, GFP-Snc1p, GFP-Sso1p or Ste2p-GFP from centromeric plasmids were grown to mid-log phase at 30 °C. The α-factor receptor Ste2p, normally expressed only on *MAT*a cells, is internalized in these *MAT*α cells, because they themselves produce α-factor and because the receptor is overexpressed. (c) Stress-induced endocytosis of Can1p is normal. WT and yyΔΔ cells harboring pCAN1-GFP were grown to exponential phase and resuspended in glucose-free medium. 0, 30 or 60 min later the cells were collected and viewed.

cell surface in yyΔΔ cells and evaluation of data showed no statistically differences in subcellular localization of Gas1p and Pma1p between WT and yyΔΔ cells. This argued that in yyΔΔ cells the sphingolipid rich rafts in the ER form correctly.

The yeast plasma membrane is known to comprise several subdomains, which are enriched for specific sets of membrane proteins, namely the dotty membrane compartment of Can1p (MCC), the meshlike compartment of Pma1p (MCP) and the dotty compartment of TORC2 (MCT). The dotty MCC contains the proton symporters Can1p, Tat2p and Fur4p, carrying arginine, tryptophan and uracil, respectively, and several other membrane proteins; the MCC colocalizes with and is stabilized by the underlying eisosomes (Malinska *et al.*, 2003; Grossmann *et al.*, 2008). Importantly, genetic and pharmacological data indicate that sphingolipids and ergosterol are important for the maintenance of the MCC and of eisosomes (Grossmann *et al.*, 2008; Fröhlich *et al.*, 2009). As can be seen in Fig. 2a, Can1p-GFP and Fur4p-GFP showed the typical spotty appearance in the plasma membrane indicating their proper integration into the MCC also in yyΔΔ. In contrast, Pma1p showed the typical homogenous distribution of the PMP. Thus, alkaline ceramidases do not seem to be required for surface transport of GPI proteins and multi-span plasma membrane proteins nor their segregation into subdomains.

Intracellular trafficking pathways in yyΔΔ cells are normal

As sphingolipids also regulate intracellular protein targeting and as these processes determine the morphology of organelles, we surveyed organellar morphology by introducing into the yyΔΔ background mtGPF, GFP-Vph1p, GFP-Sec63p, RFP-Sec7p and GFP-Sed5p for life staining of mitochondria, vacuoles, ER, *trans*-Golgi and *cis*-Golgi, respectively. As shown in Fig. S1, the morphology of all these compartments was perfectly normal in yyΔΔ cells. We also checked intracellular trafficking routes in yyΔΔ cells more directly by monitoring the distribution of proteins, which are continuously commuting between organelles. Observation of the Golgi v-SNARE Snc1p-GFP assesses the traffic from endosomes to the plasma membrane and back. In WT cells, GFP-Snc1p primarily labels the plasma membrane as well as small internal punctate structures that correspond to early endosomes and *trans*-Golgi structures (Lewis *et al.*, 2000). No difference was found between yyΔΔ and WT cells (Fig. 2b). The corresponding plasma membrane t-SNARE GFP-Sso1p was also distributed normally in yyΔΔ cells (Fig. 2b).

Phm5p is a vacuolar enzyme known to transit from the Golgi to the vacuole directly via endosomes and the multivesicular body (MVB) pathway (Dunn *et al.*, 2004). Phm5p-GFP was correctly targeted to the vacuolar lumen in yyΔΔ cells (Fig. 2b) indicating that the MVB pathway was functioning correctly. Furthermore, Ste2p-GFP, the yeast α-mating factor receptor, which undergoes endocytosis and trafficking to the vacuole in a ligand-dependent fashion (Stefan & Blumer, 1999) was internalized normally in yyΔΔ cells (Fig. 2b).

Constitutive and stress-induced endocytosis is normal in yyΔΔ cells

Normal and stress-induced endocytosis of plasma membrane proteins can be induced and regulated by LCBs, and this explains why exogenously added PHS can inhibit the growth of auxotrophic cells requiring nutrient transporters at their surface (Chung *et al.*, 2000, 2001; Zanolari *et al.*, 2000). As shown in Fig. S2a, the membrane seeking fluorescent dye FM4-64 entered yyΔΔ cells via endosomes and reached the vacuolar membrane at a normal rate, that is, within 45 min. Similarly, the water-soluble fluorescent dye Lucifer Yellow was taken up by yyΔΔ cells at a normal rate (Fig. S2b).

As shown in Fig. 2c, upon acute glucose starvation of WT cells Can1p-GFP appeared in endosomes after 30 min and in vacuoles after 60 min and endocytosis of Can1p-GFP followed the same kinetics in yyΔΔ cells, demonstrating that stress-induced endocytosis of nutrient transporters is unaffected in yyΔΔ cells. Other kinds of stress such as an inhibition of protein synthesis or heat shock were also tested as stimuli for Can1p endocytosis. While all these agents could trigger rapid endocytosis of Can1p, no difference between WT and yyΔΔ could be observed (not shown).

ISC1 encodes a hydrolase for IPC, MIPC and $M(IP)_2C$ and *isc1*Δ contain significantly increased amounts of these complex sphingolipids when metabolically labeled with [^{3}H]DHS (Sawai *et al.*, 2000). *Isc1*Δ have also been shown to secrete a small fraction of vacuolar enzymes such as CPY (Bonangelino *et al.*, 2002). Although similar labeling experiments also showed a significant increase in complex sphingolipids in yyΔΔ cells (Mao *et al.*, 2000b), yyΔΔ did not secrete the vacuolar carboxypetidase CPY (Fig. S3a).

Detergent resistance of lipid raft proteins

As mentioned, the bulk of Gas1p, Can1p, Fur4p and Pma1p are typically found in detergent resistant membranes, but become detergent extractable when sphingolipid biosynthesis is compromised (Bagnat *et al.*, 2000). To directly test if the loss of ceramidase function affects the association of these proteins with lipid rafts, cell membranes of yyΔΔ cells were incubated with 1% of Triton X-100 at 4 °C for 30 min and then loaded at the bottom of a stepwise density gradient (Bagnat *et al.*, 2000). Solubilized proteins remain at the bottom of the tube during the following ultracentrifugation, while detergent resistant membranes float to the top. We find that Gas1p and Can1p are still floating in yyΔΔ cells, albeit somewhat less rapidly than in WT cells (Fig. S3b).

Detergent resistance of membrane proteins can also be probed simply by extracting them with different concentrations of nonionic detergent. Indeed, Can1p resists extraction at low detergent concentrations in WT cells but not so in mutants, in which the MCC compartment is destabilized (Grossmann *et al.*, 2008). As shown in Fig. 3a, detergent resistance of Can1p-GFP was the same in yyΔΔ as in WT cells.

We also used a strain, in which *YPC1* was overexpressed. In this yyΔΔ.YPC1 strain, Can1p-GFP was more resistant to detergent extraction than in WT (Fig. 3a).

We therefore asked the question whether the increased detergent resistance of Can1p in yyΔΔ.YPC1 cells protect Can1p from being endocytosed. Increased stability of Can1p in the plasma membrane has been shown to lead to an increased sensitivity to canavanine, a toxic arginine analogue that enters the cell via Can1p, and canavanine sensitivity therefore formed the bases for genetic screens to discover regulators of Can1p-endocytosis (Lin *et al.*, 2008). As shown in Fig. 3b, WT and yyΔΔ cells display the same moderate sensitivity to canavanine but overex-

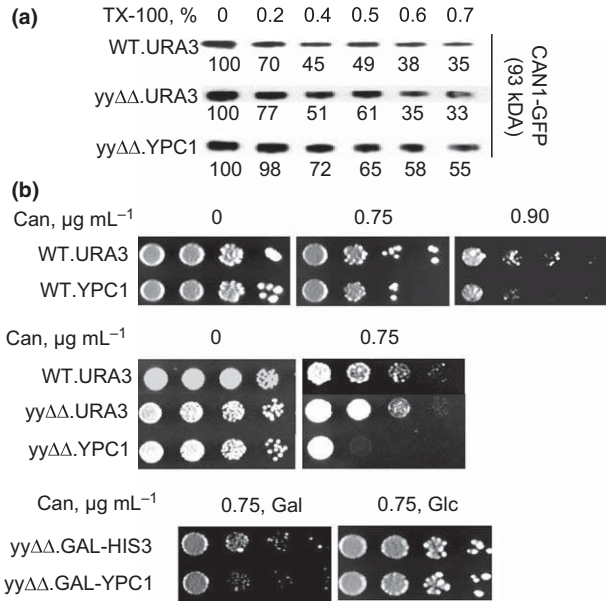

Fig. 3. (a) Association of Can1p with detergent resistant membranes in yyΔΔ and *YPC1* overexpressing cells. WT and yyΔΔ containing empty vector (WT.URA3 or yyΔΔ.URA3 respectively) and yyΔΔ with *YPC1* behind the *ADH1* promoter (yyΔΔ.YPC1) were grown to exponential phase. Membrane proteins (50 μg per sample) were treated with increasing concentrations of Triton X-100 for 30 min at room temperature exactly as described (Grossmann *et al.*, 2008). After high speed centrifugation, the nonsolubilized proteins of the pellet were resolved by SDS-PAGE and detected by specific antibodies on Western blots. Percent of detergent resistant Can1p-GFP was calculated as compared with the nontreated sample and indicated below the bands. (b) *YPC1* overexpression makes cells canavanine hypersensitive. WT and yyΔΔ cells with *YPC1* behind the *ADH1* (top panels) or the *GAL1* promoter (bottom panel) were grown to exponential phase and were serially diluted on the medium containing canavanine or solvent. Cells were incubated at 30 °C for 3 days.

pression of *YPC1* makes cells more sensitive to canavanine. The same was observed when *YPC1* was overexpressed from a *GAL1* promoter (Fig. 3b, bottom). These results are unexpected as overexpression of *YPC1* would be expected to increase LCB levels, which are known to destabilize the transporters and promote their endocytosis and this ought to make cells canavanine-resistant rather than hypersensitive (Chung *et al.*, 2000). One speculative explanation would be that local LCB and free fatty acid concentrations at the plasma membrane may allow Ypc1p to work in the reverse direction, thereby reducing LCB and increasing ceramide levels.

Cells lacking alkaline ceramidases have a normal sphingolipid composition

Metabolic labeling with [^{14}C]serine demonstrated that yyΔΔ cells accumulated the same ceramide species as WT cells (Fig. S4a). The same was true also after treatment with AbA, a cyclic depsipeptide antifungal antibiotic, which inhibits the IPC synthase Aur1p, thereby causing accumulation of ceramides (Endo *et al.*, 1997; Nagiec *et al.*, 1997; Fig. S4a). AbA treatment caused a drastic reduction of labeling of IPCs, and to a lesser degree, of MIPCs and M$(IP)_2$Cs, as expected (Fig. S4b). When analyzed by mass spectrometry, no significant difference in any class of sphingolipid was observable between WT and yyΔΔ cells (Fig. 4a). Treatment with AbA for 4 h again led to the expected drastic increase of ceramide levels and a marked reduction of IPC, MIPC and M$(IP)_2$C levels (Fig. 4a). (The reduction of IPCs under AbA is more pronounced than that of MIPC and M$(IP)_2$C, as not only caused by dilution of IPCs during a further cell division but mainly by the further maturation of premade IPC to MIPC and M$(IP)_2$C.) When analyzing the different species containing 42–46 carbon atoms and three or four hydroxyl groups in their ceramide moiety, the profile of yyΔΔ cells was the same as the one of WT (not shown). These findings are apparently in contrast to the earlier observed marked increase of all complex sphingolipids observed in *ypc1*Δ and yyΔΔ cells labeled with [^{3}H]C16:0 (Mao *et al.*, 2000a, b). The discrepancy may be explained by the fact that our mass spectrometric method fails to detect the ceramides with C14 and C16 fatty acids, as they are two or three orders of magnitude less abundant than those with C24 and C26 (Montefusco *et al.*, 2013, 2014), and secondly by assuming that the sphingolipids previously observed after labeling with [^{3}H]C16:0 contained nonelongated [^{3}H]C16:0 and hence were derived from these minor ceramides. It also may be that there are different ceramide pools and that only ceramides made from fatty acids taken up from the medium are substrates for Ypc1p and Ydc1p. Overall, at their physiological expression levels, Ypc1p and Ydc1p do not seem to be able to reduce the levels of the major C26:0-containing ceramides accumulating under AbA.

yyΔΔ cells grow normally on aureobasidin A and high concentrations of PHS

In spite of these results, we wondered if Ypc1p and Ydc1p could mitigate the toxicity of ceramides that accumulate when cells are exposed to AbA. As shown in Fig. 4b, high concentrations of AbA killed the yyΔΔ cells no faster than WT cells and no viable cells remained after 5 h of treatment. Also, on low concentrations of AbA, yyΔΔ cells were not growing less well than WT (Fig. 4c). Overexpression of *YPC1* rendered cells more resistant to high concentrations of PHS in the culture medium (Mao *et al.*, 2000b), an effect believed to be due to an increased ceramide biosynthesis through reverse ceramidase activity. This suggests

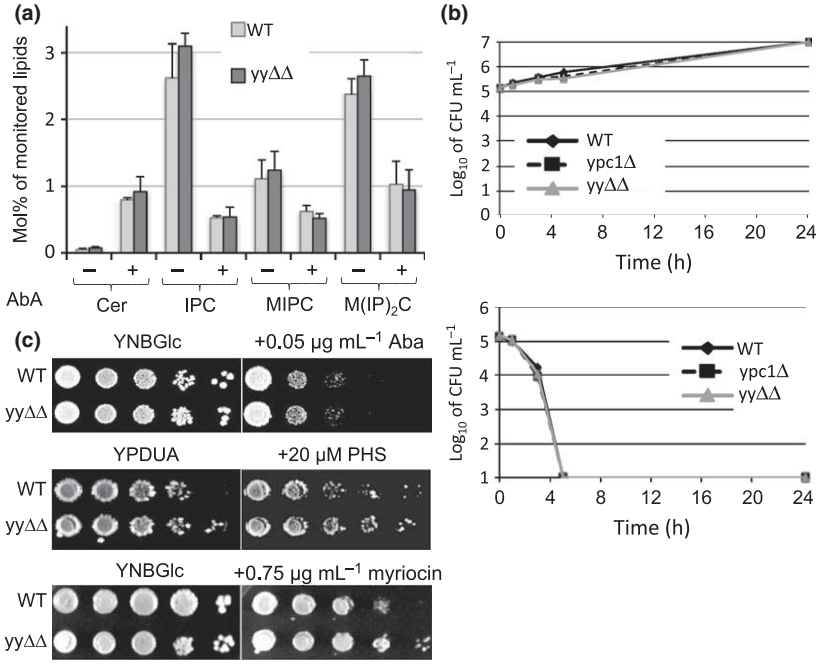

Fig. 4. Sphingolipid levels and sensitivity to AbA are not altered in yyΔΔ cells. (a) WT and yyΔΔ cells growing exponentially at 30 °C and reaching a density of OD_{600} = 0.4–0.6 were either extracted directly or further incubated in the presence of AbA (0.25 μg mL^{-1}) for 4 h during which time they reached an OD_{600} of 1.0–1.6. Lipids from treated and nontreated cells were subjected to lipidomic analysis. Bars indicate standard deviations of four determinations (two biological replicates each run twice). (b) *ypc1*Δ, yyΔΔ and WT cells were grown till exponential phase. 10^5 cells were suspended in fresh synthetic medium containing 5.0 μg mL^{-1} of AbA (bottom panel) or not (top panel). Cells were further incubated at 24 °C, and viability was measured at 0, 1, 3, 5 and 24 h by plating an aliquot of cells onto YPD. Duplicate preparations were examined. After culture for 3 days at 30 °C, CFUs were counted. (c) WT and yyΔΔ cells were grown till exponential phase and then replicated by serial 10-fold dilution on media supplemented or not with AbA, PHS or myriocin. Plates were incubated at 30 °C for 3 days.

that yyΔΔ may be hypersensitive to PHS. However, yyΔΔ and WT cells grew at the same rate on medium supplemented with PHS. On media containing myriocin, which blocks LCB synthesis (Fig. 1) and therefore may render breakdown of ceramides unnecessary, yyΔΔ grew slightly better than WT (Fig. 4c). Overall, Ypc1p and Ydc1p, when expressed from their endogenous promoter, do not seem to have any homeostatic role when cell growth is compromised by artificially increased ceramide or LCB levels.

In vivo substrate specificity of the reverse ceramidase activity of Ypc1p

To characterize the ceramides that potentially could be generated locally in the ER by *YPC1*-dependent reverse ceramidase activity, *in vivo* we analyzed the sphingolipid profile of *lag1*Δ*lac1*Δ cells overexpressing *YPC1* (2Δ.YPC1) by LC-MS/MS. The 2Δ.YPC1 strain is only viable as long as it harbors the multicopy plasmid carrying *YPC1* and all its ceramides are made by Ypc1p (and endogenous Ydc1p). As shown in Fig. 5a, the parental YPK9 cells only make IPCs and MIPCs with 42, 44 or 46 C atoms and mostly four or three hydroxyl groups in their ceramide moiety, quite in agreement with the literature. (DHS and PHS are counted as contributing two and three hydroxyls, respectively, the remaining hydroxyl groups residing on the fatty acid moiety.) As the most abundant yeast sphingolipids contain PHS with 18, less frequently 20 carbon atoms, the predominance of IPC44 and IPC46 suggests that the sphingolipids of YPK9 WT cells most frequently contain C26:0 fatty acids and their mono-hydroxylated derivatives. According to the sphingolipid profile shown in Fig. 5a and b, 2Δ.YPC1 cells contain much lower amounts of IPCs and MIPCs than WT cells, but they also predominantly make IPC44 and IPC46 species, although IPC42 and IPC40 species represent a higher fraction of total IPCs than in parental YPK9 cells. In all cells, basically only IPC44 and IPC46 are used for MIPC biosynthesis (Fig. 5b). For unknown reasons, all sphingolipid classes of 2Δ.YPC1 contain relatively more species with three than with four hydroxyls, while the reverse is true in WT cells. In summary, the profile of sphingolipids of 2Δ.YPC1 suggests that Ypc1p *in vivo* preferentially uses very long chain fatty acids.

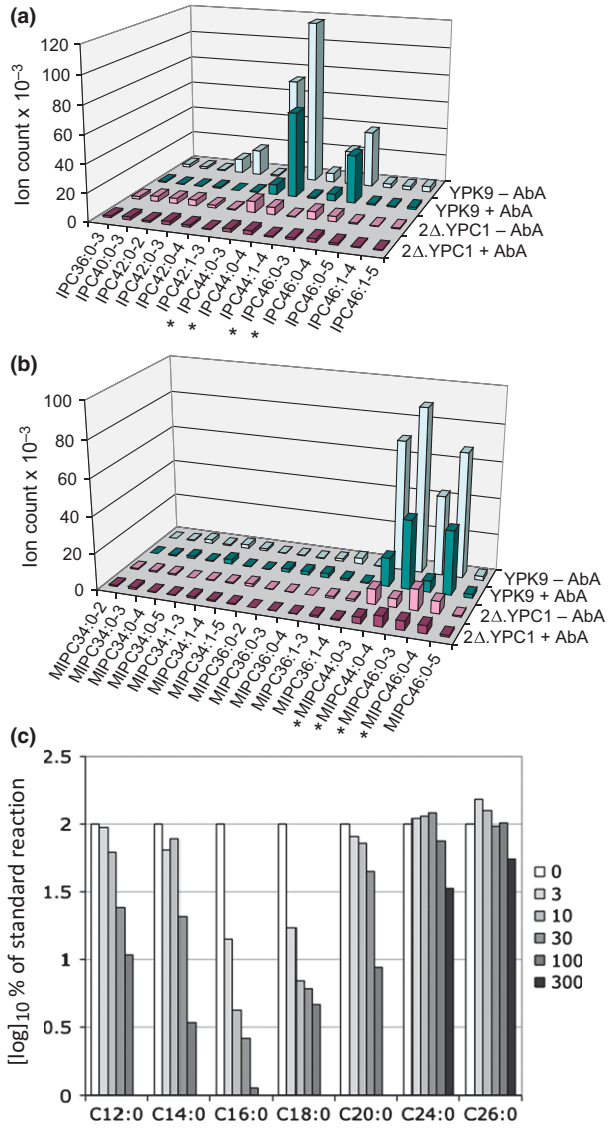

Fig. 5. Ypc1p uses different fatty acids for reverse activity *in vivo* than *in vitro*. (a, b) Cells growing exponentially in YPG at 30 °C were diluted into fresh medium supplemented or not with AbA (1 μg mL^{-1}) and further incubated at 30 °C for 4 h. Lipid extracts were deacylated using NaOH and analysed by LC-MS/MS. Of all theoretically possible species only those are plotted, for which corresponding ions were detectable in at least one strain. Sphingolipids are specified by three consecutive figures (X:Y-Z), X, Y and Z standing for the number of C atoms, number of double bonds and number of hydroxyls in their ceramide moiety, respectively. (c) Microsomal Triton X-100 extracts from 1Δ.YPC1 cells were incubated under the same conditions as used in the original report (Mao *et al.*, 2000b) with 2 μCi (0.3 nmol) of [^{3}H]C16:0 and 5 nmol PHS to measure reverse ceramidase activity. Various amounts of nonlabeled fatty acids (0–300 nmol) were added as competitors. Lipid extracts were separated by TLC and radioscanning of the TLC plates allowed to calculate the ratio of counts in ceramide (PHS[^{3}H]C16:0) over counts in the whole lane. Without competitors, this percentage was 8.0% of total radioactivity in the lane. The PHS-[^{3}H]C16:0 formed in reactions containing competitors was expressed as a percentage of PHS-[^{3}H]C16:0 in the basic reaction devoid of competing fatty acids and plotted on a $\log_{10}$ scale.

In vitro substrate specificity of the reverse ceramidase activity of Ypc1p

The original standard assay of reverse ceramidase of Ypc1p activity utilizes [^{3}H]C16:0 and PHS as substrates (Mao *et al.*, 2000b). We tried to elucidate the fatty acid specificity of this assay by adding different concentrations of unlabeled fatty acids of variable chain length as competitive inhibitors. This demonstrated that C16:0 was by far the best competitor, and hence, the best substrate compared with shorter and longer fatty acids (Fig. 5c). Also unsaturated and alpha-hydroxylated fatty acids, which are not made by yeast cells but may be taken up from the surroundings, are not better substrates for Ypc1p than C16:0 (Fig. S5a). Thus, the *in vitro* test does not seem to reflect the situation *in vivo*, as discussed below.

Previous studies have shown that *lcb1*Δ mutants can take up and utilize not only the physiological D-*erythro* but also L-*threo* forms of LCBs, which latter are transformed *in vivo* into D-*erythro* type LCBs (Watanabe *et al.*, 2002). Neither L- nor D-*threo* forms of DHS could be utilized efficiently in the standard assay (Fig. S5b), suggesting that L-*threo* DHS could not be transformed into D-*erythro* DHS *in vitro*. On the other hand, D-sphingosine, the predominant LCB in mammalian sphingolipids, was a good substrate for reverse ceramidase activity, although a sphingosine containing ceramide was not hydrolyzed in the microsomal ceramidase assay of Ypc1p in the original report (Mao *et al.*, 2000b).

Testing mitochondrial functions of yyΔΔ

Recent data have shed light on the role of a previously unsuspected mitochondrial metabolism of sphingolipids. During diauxic shift Isc1p moves from the ER to the outer membrane of mitochondria (Vaena de Avalos *et al.*, 2004), where it causes an increase of α-hydroxylated phytoceramide, which is believed to be a precondition for the postdiauxic induction of genes involved in aerobic carbon metabolism (Kitagaki *et al.*, 2007, 2009). Moreover, deletion of *ISC1* increases iron levels, reactive oxygen species, oxidative stress markers and H_2O_2 sensitivity of cells, and thereby causes premature aging, that is increased apoptosis and a drastic reduction of the chronological life span (CLS; Almeida *et al.*, 2008). Similarly, *ypc1*Δ cells were found to be hypersensitive to 2–5 mM H_2O_2 (Higgins *et al.*, 2002; Hillenmeyer *et al.*, 2008). In view of this, we decided to test mitochondrial function in

yyΔΔ cells. Contrary to *isc1*Δ cells (Vaena de Avalos *et al.*, 2005), yyΔΔ showed normal growth on all nonfermentable carbon sources tested (Fig. S6).

One sign of oxidative stress in cells is an increased protein carbonylation (Costa *et al.*, 2002). Protein carbonyls can be quantitated after derivatization with 2,4-dinitrophenylhydrazine. As can be seen in Fig. S7, after an H_2O_2 stress most carbonylated proteins were found in the membrane fractions but protein carbonylation did not appear to be increased in yyΔΔ cells as compared to WT. In summary, while cells lacking alkaline ceramidases are reported to be H_2O_2 hypersensitive, their mitochondrial respiration does not seem to be compromised and complete absence of alkaline ceramidases does not influence the protein carbonylation upon H_2O_2 stress.

Deletions of *YPC1* and *YDC1* affect CLS

Numerous recent studies suggest a link between changes in sphingolipid metabolism, oxidative stress resistance and life span (Aerts *et al.*, 2006; Almeida *et al.*, 2008; Huang *et al.*, 2012, 2013; Lester *et al.*, 2013). In particular, it was found that during chronological aging, ceramide synthase activity and LCB kinase activities decline more rapidly than LCB synthesis, leading to a drastic increase of LCB levels (Lester *et al.*, 2013). Moreover, it was shown that low concentrations of myriocin, reducing LCB, ceramide and IPC concentrations (Fig. 1) could significantly enhance CLS through complex regulatory mechanisms including reduced signaling through TORC1-Sch9p, but also through other pathways (Huang *et al.*, 2012, 2013). Finding no physiological function for Ypc1p and Ydc1p in exponentially growing cells, we wondered if such a function may be required in postdiauxic cells, in which *YPC1* mRNA strongly increases (Gasch *et al.*, 2000). Indeed, it had been reported that stationary *ydc1*Δ (but not *ypc1*Δ) cells kept at 30 °C in synthetic complete medium had a prolonged CLS (Powers *et al.*, 2006). Quite to the contrary, a recent study showed that *ydc1*Δ cells had a > twofold reduced CLS in synthetic complete medium (Laschober *et al.*, 2010). Here, we tested the longevity of yeast cells transferred from a postdiauxic culture into water according to a commonly used protocol, which, compared to other assays, reduces pH effects of the medium, prevents feeding of starved cells on remains from dead cells, and additionally imposes caloric restriction on cells (Almeida *et al.*, 2008; Longo *et al.*, 2012). As can be seen in Fig. 6a, when postdiauxic cells were transferred to water, *ydc1*Δ had a shortened, *ypc1*Δ and yyΔΔ cells a prolonged CLS. The same tendencies were also observed in an experiment performed under different conditions (Fig. S8). Thus, these studies confirmed the results of (Laschober *et al.*, 2010) concerning *ydc1*Δ mutants and suggested that *ypc1*Δ had a prolonged CLS (Fig. 6a). When cells having been in water for prolonged periods were placed back into rich medium, WT and yyΔΔ cells had the same lag phase before resuming exponential growth (not shown). Further studies also showed that *ypc1*Δ, *ydc1*Δ and yyΔΔ cells were not different from WT with regard to sporulation and germination efficiency during the first 10 days after sudden starvation inducing sporulation (not shown).

Ypc1p is localized to cortical ER

Ypc1p-GFP and Ydc1p-GFP have been described to be located in the ER when strongly overexpressed from a

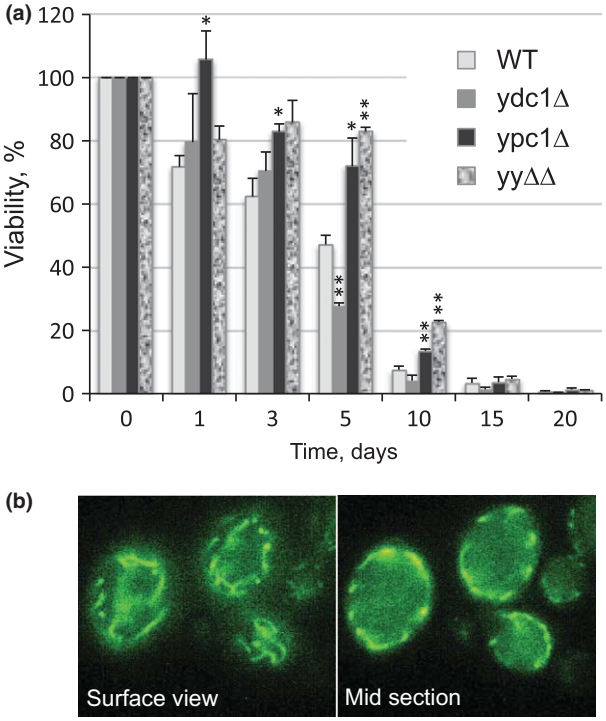

Fig. 6. Effect of deletions of *YPC1* and *YDC1* on chronological life span. (a) WT, *ypc1*Δ, *ydc1*Δ and yyΔΔ mutants were grown in YPD to stationary phase (OD_{600} of 10). After 36 h, they were washed and resuspended in H_2O and left at 30 °C on a rotating wheel according to a protocol adapted from Longo *et al.* (2012). Cells were re-washed with sterile water every 2 days. Their viability was determined at different time intervals by plating and counting colony-forming units (CFU). Results were expressed as percentages of CFUs present at time 0 h. Data are means with SD of four different biological replicates (two from BY4741 and two from BY4742 background except for *ydc1*Δ*ypc1*Δ which represents only two biological replicates in BY4742 background). *P*-values when compared to WT are indicated (*$P < 0.05$, **$P < 0.005$). (b) Diploid FY1679.YPC1-GFP cells harboring a centromeric plasmid with a *YPC1*-GFP fusion expressed from the constitutive *TEF1* promoter were grown to stationary phase and viewed under the fluorescence microscope. Surface view (left) and cross-section (right) of the same cells are shown. Over 90% of the 100 cells inspected displayed this distribution of Ypc1p-GFP.

2 μ vector and placed behind the *GAL1* promoter (Mao *et al.*, 2000b). Expressed from a centromeric vector under the *TEF1* promoter, Ypc1p-GFP was found mainly in vesicles and the nuclear membrane (http://ypl.uni--graz.at/pages/home.html; Natter *et al.*, 2005). Using the same diploid yeast strain containing Ypc1p-GFP as Natter *et al.* had used for their high-throughput localization effort, we found that Ypc1p-GFP was exclusively present in the cortical ER in stationary cells (Fig. 6b). Ypc1p-GFP was mostly localized at the cell periphery also in exponentially growing cells (Fig. S9). ER localization seems to be preserved even though the C-terminal, cytosolically located KKXX ER retrieval motif is obfuscated by the addition of GFP. It is noteworthy that Ypc1p does not contain any SMP domains as is the case for the prototypic Ist2p, which is confined to the cortical ER because it interacts in trans with PI4,5-P_2 on the plasma membrane (Manford *et al.*, 2012).

Discussion

An ancestral alkaline ceramidase gene was duplicated during the ancient whole gene duplication event in *Saccharomyces*, and the genomic regions of *YPC1* and *YDC1* were among the few genome regions that were both preserved during the ensuing genome reduction (Wolfe & Shields, 1997). *YPC1* belongs to a gene family characterized by a conserved motif (pfam05875), which has members in fungi, plants and vertebrates, including humans. Exponentially growing WT yeast cells contain readily detectable microsomal Ypc1p activity (see Introduction). Yet, our studies revealed little phenotypes in cells lacking one or both of these genes and even failed to reproduce one of the most interesting phenotypes described for *ypc1*Δ cells, the missorting of Mid-Fus-GFP (Proszynski *et al.*, 2005). Indeed, by all criteria used, the morphology of intracellular organelles and the trafficking of proteins through the secretory pathway were found to be normal in yyΔΔ cells. The only phenotype related to protein trafficking was observed when *YPC1* was overexpressed (Fig. 3). In this case, the association of the multispan integral membrane protein Can1p with detergent resistant membranes was increased and its endocytosis correspondingly decreased (Grossmann *et al.*, 2008), although levels of the major sphingolipids of such *YPC1* overexpressing cells do not change significantly (N. S. Voynova and H. M. Vazquez, manuscript in preparation). Thus, these data suggest that ceramide turnover or synthesis catalysed by overexpressed *YPC1* may alter sphingolipid composition of the plasma membrane in a way that endocytosis of proteins located in the MCC is reduced, but the reason for this phenomenon is presently elusive.

Genetic interactions as measured by SGA analysis mainly reflect fermentative growth rate of cells and the general absence of genetic interactions of yyΔΔ cells with third party genes indicates that Ypc1p and Ydc1p do not become important for fermentative growth of cells, even when they are stressed by the deletion of further genes. In keeping with this, we did not detect any abnormality in the sphingolipid profile of fermentatively growing cells (Fig. 4a). Our results are in contrast to a study in *Drosophila* where deletion of the alkaline ceramidase Dacer led to an about twofold increase in all major ceramides, both in adult flies and pupae. Deletion of Dacer also concomitantly increased CLS, the resistance to oxidants (Paraquat) and ATP levels, especially in old flies (Yang *et al.*, 2010). It is possible that the presence or absence of ceramidases only becomes pertinent in cells having entered G_0 phase.

Contrary to *isc1*Δ cells, which show decreased levels of mitochondrial ceramide levels (Kitagaki *et al.*, 2007), one would anticipate that the yyΔΔ double deletion would rather have normal or elevated levels of mitochondrial ceramides. Thus, it is not unexpected that yyΔΔ do not have any problem with retro-signaling and grow well on nonfermentable carbon sources. *YPC1* overexpression may reduce mitochondrial ceramide levels and indeed, a recent report shows that deletion of *ISC1* and overexpression of *YPC1* have the same effect in that they both induce hypersensitivity to hydroxyurea (Matmati *et al.*, 2013). Further investigations are required to see if deletion of *YPC1* and *YDC1* antagonizes the negative effects of *ISC1* deletion on mitochondrial sphingolipid homeostasis and retro-signaling.

The sphingolipid profile of 2Δ.YPC1 cells (Fig. 5a) shows a predominance of IPCs containing C24 and C26 fatty acids, quite in contrast to the one of *lag1*Δ*lac1*Δ cells overexpressing *YDC1* (2Δ.YDC1), where the ion counts for IPCs with C18, C20, C22, C24 and C26 were roughly comparable (Cerantola *et al.*, 2009). Going by the assumption that the profile of free fatty acids in all *lag1*Δ*lac1*Δ cells is the same, it would appear that Ypc1p has a preference for very long chain fatty acids, while Ydc1p has a broader specificity. It is not clear why the *in vitro* reverse ceramidase assay does not reflect the *in vivo* preference of Ypc1p. It is possible that the *in vitro* assay, beyond enzyme specificity, also measures the rate of fatty acid exchange between different detergent micelles, thus privileging shorter fatty acids. On the other hand, Ypc1p may reside in membrane domains enriched in C24:0 and C26:0. Ypc1p has its active site on the luminal side of the ER (Ramachandra & Conzelmann, 2013), and the concentrations of various fatty acids in the luminal leaflet of the ER are presently not known. We could not detect IPCs with a C16:0 as fatty acid after growing 2Δ.YPC1 cells in medium containing C16:0 (not shown).

The preference for C24:0 and C26:0 of the ceramide synthase activity of overexpressed *YPC1* sheds some light on

the previous report showing that overexpression of *YPC1* has biological effects. Overexpression of *YPC1* has been proposed to make cells resistant to high concentrations of PHS in the medium by lowering free PHS levels through reverse activity (Mao *et al.*, 2000b); Ypc1p thus may channel PHS into C26-containing complex sphingolipids. On the other hand, a recent report also shows that a large panel of less abundant phytoceramides containing nonhydroxylated fatty acids with 14–26 C atoms accumulate when cells are growing in presence of hydroxurea, and that their accumulation is significantly reduced by overexpression of *YPC1* (Matmati *et al.*, 2013). This strongly suggests that such ceramides are broken down by overexpressed *YPC1,* and that ceramidase activity *in vivo* is by no means restricted to ceramides with very long chain fatty acids.

The fact that the prolonged life span of *ypc1*Δ cells was not seen in a previous study (Powers *et al.*, 2006) is probably due to the fact that cells were aged in very different types of media (synthetic complete vs. water; Longo *et al.*, 2012). A recent report also found a much higher increase of the CLS in the BY genetic background when cells were transferred to water rather than kept in synthetic complete medium (Huang *et al.*, 2013). Interestingly, this increase of the CLS was induced by a combined treatment with myriocin plus rapamycin, a treatment that is predicted to curb the drastic increase of LCBs occurring during chronological aging (Lester *et al.*, 2013). The observed prolongation of CLS in *ypc1*Δ and yyΔΔ cells thus may also be caused by a relative decrease of LCBs, but it indirectly argues that the loss of *YPC1* could provide a selective advantage. Interestingly, deletion of *YDC1* strongly reduces CLS in complete synthetic media (Laschober *et al.*, 2010), and this is also seen when cells are under caloric restriction (Figs 6a and S8), suggesting that the role of *YPC1* and *YDC1* in the context of CLS is antagonistic. This antagonism also is supported by the observation that deletion of *YPC1* and *YDC1,* respectively, increase and decrease the sensitivity to H_2O_2 (Hillenmeyer *et al.*, 2008).

The scarcity of phenotypes observed in yyΔΔ cells suggests that *YPC1* and *YDC1* are not needed for growth of BY4742 in conventional media and even may not be functionally redundant. While *YPC1* may be of importance for cell survival under H_2O_2 stress its wide conservation in fungi, plants and vertebrates raises the possibility that it may also be required under other stresses or biological processes that are yet to be discovered.

Acknowledgements

We thank Hans Kristian Hannibal-Bach for running the mass spectrometric analysis, Claudio De Virgilio, Akihiko Nakano, Klaus Natter, Lauro Popolo, Fulvio Reggiori, Roger Schneiter, and Kai Simons for strains and plasmids. This work was supported by grants CRSI33_125232 and 31003AB_131078 from the Swiss National Science Foundation.

Authors' contribution

N.S.V. and S.K.M. contributed equally to this work.

References

Aerts AM, Francois IE, Bammens L, Cammue BP, Smets B, Winderickx J, Accardo S, De Vos DE & Thevissen K (2006) Level of M(IP)2C sphingolipid affects plant defensin sensitivity, oxidative stress resistance and chronological life-span in yeast. *FEBS Lett* **580**: 1903–1907.

Almeida T, Marques M, Mojzita D *et al.* (2008) Isc1p plays a key role in hydrogen peroxide resistance and chronological lifespan through modulation of iron levels and apoptosis. *Mol Biol Cell* **19**: 865–876.

Bagnat M, Keranen S, Shevchenko A, Shevchenko A & Simons K (2000) Lipid rafts function in biosynthetic delivery of proteins to the cell surface in yeast. *P Natl Acad Sci USA* **97**: 3254–3259.

Bonangelino CJ, Chavez EM & Bonifacino JS (2002) Genomic screen for vacuolar protein sorting genes in *Saccharomyces cerevisiae*. *Mol Biol Cell* **13**: 2486–2501.

Cerantola V, Guillas I, Roubaty C, Vionnet C, Uldry D, Knudsen J & Conzelmann A (2009) Aureobasidin A arrests growth of yeast cells through both ceramide intoxication and deprivation of essential inositolphosphorylceramides. *Mol Microbiol* **71**: 1523–1537.

Chung N, Jenkins G, Hannun YA, Heitman J & Obeid LM (2000) Sphingolipids signal heat stress-induced ubiquitin-dependent proteolysis. *J Biol Chem* **275**: 17229–17232.

Chung N, Mao C, Heitman J, Hannun YA & Obeid LM (2001) Phytosphingosine as a specific inhibitor of growth and nutrient import in *Saccharomyces cerevisiae*. *J Biol Chem* **276**: 35614–35621.

Collins SR, Roguev A & Krogan NJ (2010) Quantitative genetic interaction mapping using the E-MAP approach. *Methods Enzymol* **470**: 205–231.

Costa VM, Amorim MA, Quintanilha A & Moradas-Ferreira P (2002) Hydrogen peroxide-induced carbonylation of key metabolic enzymes in *Saccharomyces cerevisiae*: the involvement of the oxidative stress response regulators Yap1 and Skn7. *Free Radic Biol Med* **33**: 1507–1515.

DeLuna A, Vetsigian K, Shoresh N, Hegreness M, Colon-Gonzalez M, Chao S & Kishony R (2008) Exposing the fitness contribution of duplicated genes. *Nat Genet* **40**: 676–681.

Dickson RC (2010) Roles for sphingolipids in *Saccharomyces cerevisiae*. *Adv Exp Med Biol* **688**: 217–231.

Dickson RC, Sumanasekera C & Lester RL (2006) Functions and metabolism of sphingolipids in *Saccharomyces cerevisiae*. *Prog Lipid Res* **45**: 447–465.

Dittmar JC, Reid RJ & Rothstein R (2010) ScreenMill: a freely available software suite for growth measurement, analysis and visualization of high-throughput screen data. *BMC Bioinformatics* **11**: 353.

Dunn R, Klos DA, Adler AS & Hicke L (2004) The C2 domain of the Rsp5 ubiquitin ligase binds membrane phosphoinositides and directs ubiquitination of endosomal cargo. *J Cell Biol* **165**: 135–144.

Ejsing CS, Moehring T, Bahr U, Duchoslav E, Karas M, Simons K & Shevchenko A (2006) Collision-induced dissociation pathways of yeast sphingolipids and their molecular profiling in total lipid extracts: a study by quadrupole TOF and linear ion trap-orbitrap mass spectrometry. *J Mass Spectrom* **41**: 372–389.

Ejsing CS, Sampaio JL, Surendranath V, Duchoslav E, Ekroos K, Klemm RW, Simons K & Shevchenko A (2009) Global analysis of the yeast lipidome by quantitative shotgun mass spectrometry. *P Natl Acad Sci USA* **106**: 2136–2141.

Endo M, Takesako K, Kato I & Yamaguchi H (1997) Fungicidal action of aureobasidin A, a cyclic depsipeptide antifungal antibiotic, against *Saccharomyces cerevisiae*. *Antimicrob Agents Chemother* **41**: 672–676.

Fröhlich F, Moreira K, Aguilar PS, Hubner NC, Mann M, Walter P & Walther TC (2009) A genome-wide screen for genes affecting eisosomes reveals Nce102 function in sphingolipid signaling. *J Cell Biol* **185**: 1227–1242.

Gaigg B, Timischl B, Corbino L & Schneiter R (2005) Synthesis of sphingolipids with very long chain fatty acids but not ergosterol is required for routing of newly synthesized plasma membrane ATPase to the cell surface of yeast. *J Biol Chem* **280**: 22515–22522.

Gasch AP, Spellman PT, Kao CM, Carmel-Harel O, Eisen MB, Storz G, Botstein D & Brown PO (2000) Genomic expression programs in the response of yeast cells to environmental changes. *Mol Biol Cell* **11**: 4241–4257.

Grossmann G, Malinsky J, Stahlschmidt W, Loibl M, Weig-Meckl I, Frommer WB, Opekarova M & Tanner W (2008) Plasma membrane microdomains regulate turnover of transport proteins in yeast. *J Cell Biol* **183**: 1075–1088.

Hanson BA & Lester RL (1980) The extraction of inositol-containing phospholipids and phosphatidylcholine from *Saccharomyces cerevisiae* and *Neurospora crassa*. *J Lipid Res* **21**: 309–315.

Higgins VJ, Alic N, Thorpe GW, Breitenbach M, Larsson V & Dawes IW (2002) Phenotypic analysis of gene deletant strains for sensitivity to oxidative stress. *Yeast* **19**: 203–214.

Hillenmeyer ME, Fung E, Wildenhain J *et al.* (2008) The chemical genomic portrait of yeast: uncovering a phenotype for all genes. *Science* **320**: 362–365.

Horvath A, Sutterlin C, Manning-Krieg U, Movva NR & Riezman H (1994) Ceramide synthesis enhances transport of GPI-anchored proteins to the Golgi apparatus in yeast. *EMBO J* **13**: 3687–3695.

Huang X, Liu J & Dickson RC (2012) Down-regulating sphingolipid synthesis increases yeast lifespan. *PLoS Genet* **8**: e1002493.

Huang X, Liu J, Withers BR, Samide AJ, Leggas M & Dickson RC (2013) Reducing signs of aging and increasing lifespan by drug synergy. *Aging Cell* **12**: 652–660.

Kitagaki H, Cowart LA, Matmati N, Vaena de Avalos S, Novgorodov SA, Zeidan YH, Bielawski J, Obeid LM & Hannun YA (2007) Isc1 regulates sphingolipid metabolism in yeast mitochondria. *Biochim Biophys Acta* **1768**: 2849–2861.

Kitagaki H, Cowart LA, Matmati N, Montefusco D, Gandy J, de Avalos SV, Novgorodov SA, Zheng J, Obeid LM & Hannun YA (2009) ISC1-dependent metabolic adaptation reveals an indispensable role for mitochondria in induction of nuclear genes during the diauxic shift in *Saccharomyces cerevisiae*. *J Biol Chem* **284**: 10818–10830.

Laschober GT, Ruli D, Hofer E *et al.* (2010) Identification of evolutionarily conserved genetic regulators of cellular aging. *Aging Cell* **9**: 1084–1097.

Lester RL, Withers BR, Schultz MA & Dickson RC (2013) Iron, glucose and intrinsic factors alter sphingolipid composition as yeast cells enter stationary phase. *Biochim Biophys Acta* **1831**: 726–736.

Lewis MJ, Nichols BJ, Prescianotto-Baschong C, Riezman H & Pelham HR (2000) Specific retrieval of the exocytic SNARE Snc1p from early yeast endosomes. *Mol Biol Cell* **11**: 23–38.

Lin CH, MacGurn JA, Chu T, Stefan CJ & Emr SD (2008) Arrestin-related ubiquitin-ligase adaptors regulate endocytosis and protein turnover at the cell surface. *Cell* **135**: 714–725.

Longo VD, Shadel GS, Kaeberlein M & Kennedy B (2012) Replicative and chronological aging in *Saccharomyces cerevisiae*. *Cell Metab* **16**: 18–31.

Malinska K, Malinsky J, Opekarova M & Tanner W (2003) Visualization of protein compartmentation within the plasma membrane of living yeast cells. *Mol Biol Cell* **14**: 4427–4436.

Manford AG, Stefan CJ, Yuan HL, Macgurn JA & Emr SD (2012) ER-to-plasma membrane tethering proteins regulate cell signaling and ER morphology. *Dev Cell* **23**: 1129–1140.

Mao C & Obeid LM (2008) Ceramidases: regulators of cellular responses mediated by ceramide, sphingosine, and sphingosine-1-phosphate. *Biochim Biophys Acta* **1781**: 424–434.

Mao C, Xu R, Bielawska A & Obeid LM (2000a) Cloning of an alkaline ceramidase from *Saccharomyces cerevisiae*. An enzyme with reverse (CoA-independent) ceramide synthase activity. *J Biol Chem* **275**: 6876–6884.

Mao C, Xu R, Bielawska A, Szulc ZM & Obeid LM (2000b) Cloning and characterization of a *Saccharomyces cerevisiae* alkaline ceramidase with specificity for dihydroceramide. *J Biol Chem* **275**: 31369–31378.

Matmati N, Metelli A, Tripathi K, Yan S, Mohanty BK & Hannun YA (2013) Identification of c18:1-phytoceramide as the candidate lipid mediator for hydroxyurea resistance in yeast. *J Biol Chem* **288**: 17272–17284.

Montefusco DJ, Chen L, Matmati N, Lu S, Newcomb B, Cooper GF, Hannun YA & Lu X (2013) Distinct signaling roles of ceramide species in yeast revealed through systematic perturbation and systems biology analyses. *Sci Signal* **6**: rs14.

Montefusco DJ, Matmati N & Hannun YA (2014) The yeast sphingolipid signaling landscape. *Chem Phys Lipids* **177**: 26–40.

Nagiec MM, Nagiec EE, Baltisberger JA, Wells GB, Lester RL & Dickson RC (1997) Sphingolipid synthesis as a target for antifungal drugs. Complementation of the inositol phosphorylceramide synthase defect in a mutant strain of *Saccharomyces cerevisiae* by the AUR1 gene. *J Biol Chem* **272**: 9809–9817.

Natter K, Leitner P, Faschinger A, Wolinski H, McCraith S, Fields S & Kohlwein SD (2005) The spatial organization of lipid synthesis in the yeast *Saccharomyces cerevisiae* derived from large scale green fluorescent protein tagging and high resolution microscopy. *Mol Cell Proteomics* **4**: 662–672.

Powers RWR, Kaeberlein M, Caldwell SD, Kennedy BK & Fields S (2006) Extension of chronological life span in yeast by decreased TOR pathway signaling. *Genes Dev* **20**: 174–184.

Proszynski TJ, Klemm RW, Gravert M *et al.* (2005) A genome-wide visual screen reveals a role for sphingolipids and ergosterol in cell surface delivery in yeast. *P Natl Acad Sci USA* **102**: 17981–17986.

Ramachandra N & Conzelmann A (2013) Membrane topology of yeast alkaline ceramidase YPC1. *Biochem J* **452**: 585–594.

Sawai H, Okamoto Y, Luberto C, Mao C, Bielawska A, Domae N & Hannun YA (2000) Identification of ISC1 (YER019w) as inositol phosphosphingolipid phospholipase C in *Saccharomyces cerevisiae*. *J Biol Chem* **275**: 39793–39798.

Schorling S, Vallee B, Barz WP, Riezman H & Oesterhelt D (2001) Lag1p and Lac1p are essential for the Acyl-CoA-dependent ceramide synthase reaction in *Saccharomyces cerevisiae*. *Mol Biol Cell* **12**: 3417–3427.

Stefan CJ & Blumer KJ (1999) A syntaxin homolog encoded by VAM3 mediates down-regulation of a yeast G protein-coupled receptor. *J Biol Chem* **274**: 1835–1841.

Tani M & Kuge O (2010) Defect of synthesis of very long-chain fatty acids confers resistance to growth inhibition by inositol phosphorylceramide synthase repression in yeast *Saccharomyces cerevisiae*. *J Biochem* **148**: 565–571.

Tani M & Kuge O (2012) Hydroxylation state of fatty acid and long-chain base moieties of sphingolipid determine the sensitivity to growth inhibition due to AUR1 repression in *Saccharomyces cerevisiae*. *Biochem Biophys Res Commun* **417**: 673–678.

Vaena de Avalos S, Okamoto Y & Hannun YA (2004) Activation and localization of inositol phosphosphingolipid phospholipase C, Isc1p, to the mitochondria during growth of *Saccharomyces cerevisiae*. *J Biol Chem* **279**: 11537–11545.

Vaena de Avalos S, Su X, Zhang M, Okamoto Y, Dowhan W & Hannun YA (2005) The phosphatidylglycerol/cardiolipin biosynthetic pathway is required for the activation of inositol phosphosphingolipid phospholipase C, Isc1p, during growth of *Saccharomyces cerevisiae*. *J Biol Chem* **280**: 7170–7177.

Watanabe R, Funato K, Venkataraman K, Futerman AH & Riezman H (2002) Sphingolipids are required for the stable membrane association of glycosylphosphatidylinositol-anchored proteins in yeast. *J Biol Chem* **277**: 49538–49544.

Wolfe KH & Shields DC (1997) Molecular evidence for an ancient duplication of the entire yeast genome. *Nature* **387**: 708–713.

Yang Q, Gong ZJ, Zhou Y *et al.* (2010) Role of *Drosophila* alkaline ceramidase (Dacer) in Drosophila development and longevity. *Cell Mol Life Sci* **67**: 1477–1490.

Young BP, Shin JJ, Orij R *et al.* (2010) Phosphatidic acid is a pH biosensor that links membrane biogenesis to metabolism. *Science* **329**: 1085–1088.

Zanolari B, Friant S, Funato K, Sutterlin C, Stevenson BJ & Riezman H (2000) Sphingoid base synthesis requirement for endocytosis in *Saccharomyces cerevisiae*. *EMBO J* **19**: 2824–2833.

Supporting Information

Additional Supporting Information may be found in the online version of this article:

Fig. S1. The localization of mtGFP, Vph1p, Sec63p, Sec7p and Sed5p is normal in yyΔΔ cells.
Fig. S2. yyΔΔ cells show normal kinetics of endocytosis.
Fig. S3. CPY and Gas1p are targeted normally in yyΔΔ.
Fig. S4. Serine incorporation into lipids in yyΔΔ cells is qualitatively normal.
Fig. S5. (a) Hydroxylation or desaturation of fatty acids decreases their affinity for Ypc1p. (b) Long chain base specificity of Ypc1p-dependent microsomal reverse ceramidase activity.
Fig. S6. Growth of *ypc1Δ*, *ydc1Δ* and yyΔΔ cells on non-fermentable carbon sources.
Fig. S7. Protein carbonylation in the presence of H_2O_2.
Fig. S8. Chronological life span of *ypc1Δ* and *ydc1Δ* cells.
Fig. S9. Localization of Ypc1p-GFP in exponentially growing and stationary cells.
Data S1. Materials and methods.
Table S1. Yeast *Saccharomyces cerevisiae* strains.
Table S2. Plasmids.